



# Dicyanostilbene-derived two-photon fluorescence dyes with large two-photon absorption cross sections

Chibao Huang<sup>a,b</sup>, Changhua Lin<sup>b</sup>, Anxiang Ren<sup>b</sup>, Nianfa Yang<sup>a,\*</sup>

<sup>a</sup> Key Laboratory of Environmentally Friendly Chemistry and Applications of Ministry of Education, College of Chemistry, Xiangtan University, Xiangtan 411105, China

<sup>b</sup> Department of Agricultural Engineering, Yingdong Bioengineering College, Shaoguan University, Shaoguan 512005, China

## ARTICLE INFO

### Article history:

Received 13 May 2011

Received in revised form 24 July 2011

Accepted 6 August 2011

Available online 25 August 2011

### Keywords:

Dicyanostilbene

Two-photon absorption cross section

Two-photon dye

Bioimaging

## ABSTRACT

Four dicyanostilbene-derived two-photon fluorescence (TPF) dyes were synthesized as the model compounds to systematically study the effect of the dicyano and the terminal substituent on the two-photon absorption (TPA). These four compounds (**DSO**, **DCY**, **DTO** and **DPH**) exhibit very large two-photon absorption cross sections ( $\delta$ ). **DCY** (A- $\pi$ -A) with the terminal cyano group has especially high fluorescence quantum yield (0.71) and relatively large  $\delta$  (1480 GM), while **DPH** (D- $\pi$ -A) with the substituted amino group at its terminus possesses the largest  $\delta$  (2800 GM) and the longest emission wavelength (620 nm). The ideal terminal substituent should not be the alkoxy group but the substituted amino group. This class of dicyanostilbene dyes possess small molecule size, large  $\delta$  (830–2800 GM), long-wavelength emission (459–620 nm) and large Stokes shift (80–206 nm), and are ideal chromophores for TPF labels and probes.

© 2011 Elsevier B.V. All rights reserved.

## 1. Introduction

In recent years, two-photon excited fluorescence (TPF), which is based on molecular two-photon absorption (TPA), has received increasing attention for its various applications such as multiphoton fluorescence imaging and microscopy [1,2], microfabrication [3–5], three-dimensional (3D) data-storage [6,7], optical power limiting [8], up-converted lasing [9], photodynamic therapy [10,11], and for the localized release of bio-active species [12]. Presently, this demand is being matched by rapid advances in the design and synthesis of TPF dyes.

As a TPF dye for the functional materials, it must have high molecular weight to ensure the strength, toughness and excellent machinability of the material, whereas a TPF dye for bioimaging should have small molecule size, low molecular weight and high flexibility, which are indispensable to its good cell-permeability.

As is known to all, TPA cross section ( $\delta$ ) of a dye mainly depends on the rigidity of its planar  $\pi$ -conjugated skeleton, which, in turn, will inevitably weaken its cell-permeability. Therefore, for the purpose of applying dyes in bioimaging, a balance needs to be struck between increasing  $\delta$  and improving cell-permeability.

Stilbene derivatives are precisely such TPF dyes with small molecule size and moderately large  $\delta$ . Of a variety of donor–bridge–acceptor (D- $\pi$ -A) and donor–bridge–donor (D- $\pi$ -D) stilbene derivatives, the TPA properties were studied [13,14], and the values of their  $\delta$  are approximately  $\sim 400$  GM ( $1 \text{ GM} \equiv 1 \times 10^{-50} \text{ cm}^4 \text{ s}$

$\text{photon}^{-1} \text{ molecule}^{-1}$ ), which is not large enough yet for biological application. Higher values of  $\delta$  make it possible for lower dye concentrations and laser power to meet the need for recording images, which results in less background fluorescence from endogenous chromophores. This makes such chromophores interesting candidates for molecular TPF labels and probes. The substitution of the hydrogen atoms with the cyano groups on the aromatic ring can dramatically boost the  $\delta$  value of molecules [15,16].

By use of the attachment of two cyano groups to the single aromatic ring of a stilbene, a series of dicyanostilbene derivatives with a considerably large  $\delta$  were synthesized by us. Meanwhile, this two-cyano chromophore with the strong electron donor of a *N,N'*-disubstituted amino group at its extremity has been successfully employed in the design of TPF probes for  $\text{Hg}^{2+}$  and  $\text{Ag}^+$  ions [17,18]. Herein we report a few more derivatives (Fig. 1) from this class of dicyanostilbene dyes, and make a systematic study on their TPA properties so as to further extend their application in bioimaging.

## 2. Experimental

### 2.1. Materials and methods

NMR spectra were recorded on a VARIAN INOVA 400 MHz NMR spectrometer. Mass spectral determinations were made on a ESI-Q-TOF mass spectrometry (Micromass, UK). High resolution mass spectra measurements were performed on a GC-TOF mass spectrometry (Micromass, UK). Fluorescence measurements were performed on a PTI-C-700 Felix and Time-Master system. Fluorescence quantum yields were measured using standard methods

\* Corresponding author. Fax: +86 731 58293833.

E-mail address: [nfyang@xtu.edu.cn](mailto:nfyang@xtu.edu.cn) (N. Yang).

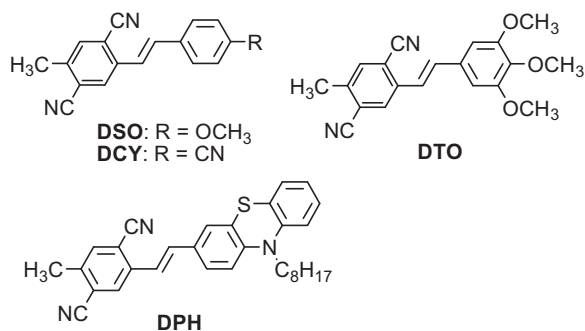


Fig. 1. Molecular structures of **DSO**, **DCY**, **DTO** and **DPH**.

[19] on air-equilibrated samples at room temperature. Quinine bisulfate in 0.05 mol L<sup>-1</sup> H<sub>2</sub>SO<sub>4</sub> ( $\Phi = 0.546$ ) was used as a reference [19]. TPEF (two-photon-excited fluorescence) action cross-section spectra were measured according to the experimental protocol established by Xu and Webb [20], using a mode-locked Ti/sapphire laser that delivers ~80 fs pulses at 76 MHz. Fluorescein (10<sup>-4</sup> mol L<sup>-1</sup> in 0.1 mol L<sup>-1</sup> NaOH), whose TPEF action cross-sections are well-known [20], served as the reference. The quadratic dependence of the fluorescence intensity on the excitation intensity was verified for each data point, indicating that the measurements were carried out in intensity regimes in which saturation or photodegradation does not occur. The measurements were performed at room temperature on air-equilibrated solutions (10<sup>-5</sup> mol L<sup>-1</sup>). The experimental uncertainty on the absolute action cross-sections determined by this method has been estimated to be  $\pm 20\%$  [20]. Absorption spectra were measured on a HP-8453 spectrophotometer. Solvents were generally dried and distilled prior to use. Reactions were monitored by thin-layer chromatography on Merck silica gel 60 F<sub>254</sub> precoated aluminum sheets. Column chromatography: Merck silica gel Si 60 (40–63  $\mu$ m, 230–400 mesh). The pH-dependent fluorescence studies were performed according to the literature [21].

## 2.2. Synthesis

### 2.2.1. General procedure of the Wittig reaction to **DSO**, **DCY**, **DTO** and **DPH**

Diethyl-2,5-dicyano-4-methylbenzylphosphonate (**5**) and the aldehyde (**6**, **7**, or **10**, 1 equiv) were suspended in about freshly distilled THF (about 50 mL), then NaH (1.2  $\pm$  1.5 equiv) in THF was added dropwise, with stirring. This procedure was carried out in an ice-bath. The mixture was continuously stirred at room temperature for a further 20 h, then poured into distilled water (200 mL). The pH value was adjusted to 7.0 by addition of 0.1 M hydrochloric acid. The product was extracted twice with CH<sub>2</sub>Cl<sub>2</sub>, and the organic layer was dried overnight over anhydrous MgSO<sub>4</sub>. The solvent was removed with a rotary evaporator to give the crude product. In order to get the desired trans compound, the crude product was isomerized by dissolving in toluene and refluxing with trace amounts of iodine for 4 h [14]. After removing the solvent, the residue was purified by column chromatography on silica gel using dichloromethane–petroleum ether (1:4) as eluent.

### 2.2.2. (E)-2-(4-methoxystyryl)-5-methylterephthalonitrile (**DSO**)

IR (KBr) cm<sup>-1</sup>: 3075 (C=C–H), 2974 (OCH<sub>3</sub>), 2923 (CH<sub>3</sub>), 2220 (C≡N), 1630 (Ar–C=C), 1598 (aromatic C=C), 1519 (aromatic C=C), 1281 (C–O), 952 (C=C–H), 804 (C=C–H), 668 (C=C–H).

HRMS (EI) *m/z*: 274.1100 (calcd for C<sub>18</sub>H<sub>14</sub>N<sub>2</sub>O: 274.1106).

Light yellow powder. Yield 82%; m.p. 212–214 °C; <sup>1</sup>H NMR (CHCl<sub>3</sub>-*d*, 400 MHz) ppm: 7.10 (s, 1H), 6.92 (s, 1H), 6.43 (d, *J* = 8.4 Hz, 2H), 6.19 (d, *J* = 16 Hz, 1H), 6.01 (d, *J* = 16 Hz, 2H), 5.84

(d, *J* = 8.4 Hz, 2H), 2.42 (s, 3H), 1.36 (s, 3H). <sup>13</sup>C NMR (CHCl<sub>3</sub>-*d*, 100 MHz) ppm: 160.00, 137.36, 131.82, 131.65, 130.26, 130.08, 129.89, 129.60, 128.28, 123.77, 123.71, 122.83, 114.32, 113.85, 55.35, 29.68.

Elemental analysis: calculated for C<sub>18</sub>H<sub>14</sub>N<sub>2</sub>O (MW 274.32): C 78.81%, H 5.14%, N 10.21%, O 5.83%; Found: C 78.93%, H 5.18%, N 10.18%, O 5.70%.

### 2.2.3. (E)-2-(4-cyanostyryl)-5-methylterephthalonitrile (**DCY**)

IR (KBr) cm<sup>-1</sup>: 3082 (C=C–H), 2925 (CH<sub>3</sub>), 2238 (C≡N), 1654 (Ar–C=C), 1596 (aromatic C=C), 1514 (aromatic C=C), 957 (C=C–H), 805 (C=C–H), 668 (C=C–H).

HRMS (EI) *m/z*: 269.0951 (calcd for C<sub>18</sub>H<sub>11</sub>N<sub>3</sub>: 269.0953).

Yellow powder. Yield 66%; m.p. 263–265 °C; <sup>1</sup>H NMR (400 MHz, CDCl<sub>3</sub>)  $\delta$ : 8.03 (s, 1H), 7.71 (d, *J* = 8.4 Hz, 2H), 7.66 (d, *J* = 8.4 Hz, 2H), 7.65 (s, 1H), 7.45 (d, *J* = 16.0 Hz, 1H), 7.28 (d, *J* = 14.4 Hz, 1H), 2.61 (s, 3H). <sup>13</sup>C NMR (CHCl<sub>3</sub>-*d*, 100 MHz) ppm: 141.91, 139.95, 137.91, 134.77, 133.09, 132.98, 132.93, 129.76, 127.86, 125.58, 118.69, 117.93, 116.46, 115.36, 112.68, 20.17.

Elemental analysis: calculated for C<sub>18</sub>H<sub>11</sub>N<sub>3</sub> (MW 269.30): C 80.28%, H 4.12%, N 15.60%; Found: C 80.35%, H 4.14%, N 15.51%.

### 2.2.4. (E)-2-(3,4,5-trimethoxystyryl)-5-methylterephthalonitrile (**DTO**)

IR (KBr) cm<sup>-1</sup>: 3068 (C=C–H), 2977 (OCH<sub>3</sub>), 2924 (CH<sub>3</sub>), 2231 (C≡N), 1650 (Ar–C=C), 1593 (aromatic C=C), 1515 (aromatic C=C), 1287 (C–O), 957 (C=C–H), 809 (C=C–H), 668 (C=C–H).

HRMS (EI) *m/z*: 334.1354 (calcd for C<sub>20</sub>H<sub>18</sub>N<sub>2</sub>O<sub>3</sub>: 334.1317).

Yellow powder. Yield 63%; m.p. 207–209 °C; <sup>1</sup>H NMR (400 MHz, CDCl<sub>3</sub>)  $\delta$ : 7.99 (s, 1H), 7.86 (s, 1H), 7.600 (s, 1H), 7.24 (d, *J* = 14.4 Hz, 1H), 6.70 (d, *J* = 16.4 Hz, 1H), 6.78 (s, 1H), 3.93 (s, 6H), 3.89 (s, 3H), 2.58 (s, 3H). <sup>13</sup>C NMR (CHCl<sub>3</sub>-*d*, 100 MHz) ppm: 160.75, 139.80, 139.33, 135.64, 134.55, 134.29, 133.49, 130.16, 129.01, 128.76, 121.94, 119.65, 117.47, 116.62, 116.56, 114.47, 55.38, 55.24, 19.88.

Elemental analysis: calculated for C<sub>20</sub>H<sub>18</sub>N<sub>2</sub>O<sub>3</sub> (MW 334.4): C 71.84%, H 5.43%, N 8.38%, O 14.35%; Found: C 71.89%, H 5.47%, N 8.37%, O 14.28%.

### 2.2.5. (E)-2-methyl-5-(2-(10-octylphenothiazin-3-yl)vinyl)terephthalonitrile (**DPH**)

IR (KBr) cm<sup>-1</sup>: 3072 (C=C–H), 2974–2857 (saturated C–H), 2922 (CH<sub>3</sub>), 2238 (C≡N), 1647 (Ar–C=C), 1592 (aromatic C=C), 1511 (aromatic C=C), 1448 (CH<sub>3</sub>), 956 (C=C–H), 808 (C=C–H), 737 (*n*-octyl), 668 (C=C–H).

HRMS (EI) *m/z*: 477.2234 (calcd for C<sub>31</sub>H<sub>31</sub>N<sub>3</sub>S: 477.2239).

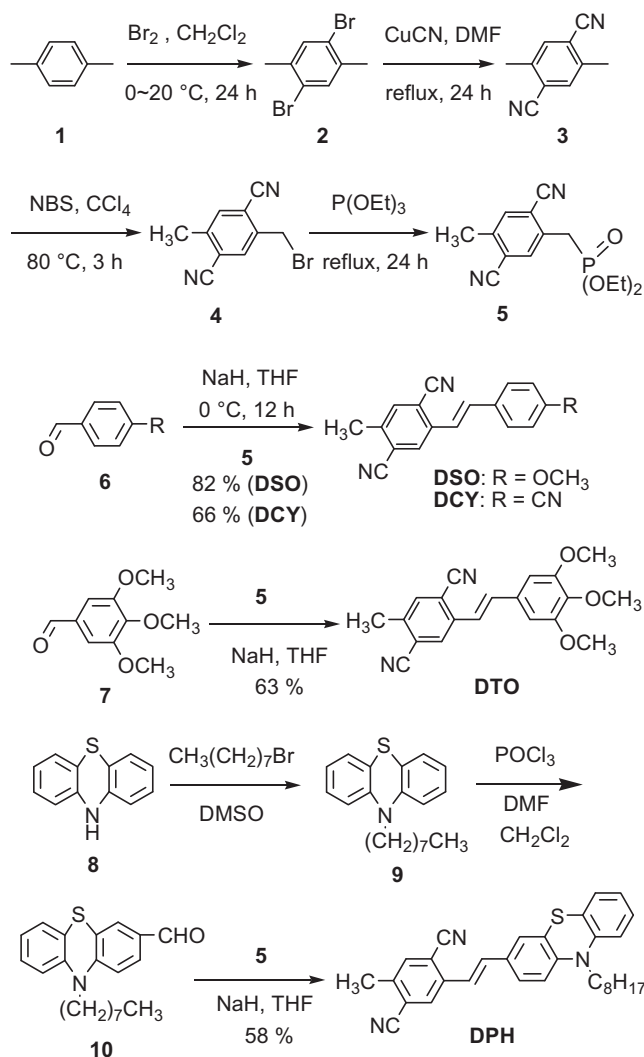
Yellow powder. Yield 58%; m.p. 238–240 °C; <sup>1</sup>H NMR (400 MHz, CDCl<sub>3</sub>)  $\delta$ : 7.96 (s, 1H), 7.57 (s, 1H), 7.32 (s, 2H), 7.14 (m, 4H), 6.85 (m, 2H), 3.87 (s, 2H), 2.57 (s, 3H), 1.81 (m, 2H), 1.44 (m, 2H), 1.28 (m, 8H), 0.87 (t, *J*<sub>1</sub> = 6.0 Hz, *J*<sub>2</sub> = 7.2 Hz, 3H). <sup>13</sup>C NMR (CHCl<sub>3</sub>-*d*, 100 MHz) ppm: 146.26, 144.44, 141.55, 140.91, 139.85, 139.14, 134.31, 133.75, 130.80, 129.88, 129.07, 127.46, 127.34, 126.72, 125.81, 124.08, 122.77, 119.85, 117.46, 116.54, 115.51, 114.31, 47.73, 45.68, 44.81, 31.71, 29.17, 26.89, 22.58, 19.88, 14.01.

Elemental analysis: calculated for C<sub>31</sub>H<sub>31</sub>N<sub>3</sub>S (MW 477.66): C 77.95%, H 6.54%, N 8.80%, S 6.71%; Found: C 78.07%, H 6.59%, N 8.71%, S 6.63%.

## 3. Results and discussion

### 3.1. Design and synthesis of **DSO**, **DCY**, **DTO** and **DPH**

2,5-Dibromo-*p*-xylene (**2**) [22], 2,5-dimethyl-terephthalonitrile (**3**) [22], 2-bromomethyl-5-methylterephthalonitrile (**4**) [18], 1-diethylphosphorylmethyl-4-methyl-2,5-dicyanobenzene (**5**) [18], 10-*n*-octylphenothiazine (**9**) [23], and 10-*n*-octylphenothiazine-3-



**Scheme 1.** Synthetic procedures of **DSO**, **DCY**, **DTO** and **DPH**.

carbaldehyde (**10**) [23] were synthesized according to literature procedures. **DSO**, **DCY**, **DTO** and **DPH** (Scheme 1) were obtained in modest yield by condensation between **5** and aldehydes **6**, **7** and **10**, respectively.

### 3.2. One-photon absorption and fluorescence spectra

One-photon absorption and fluorescence spectra of **DSO**, **DCY**, **DTO** and **DPH** in CH<sub>2</sub>Cl<sub>2</sub> solution are depicted in Figs. 2 and 3. The results indicate that the maximum absorption wavelengths ( $\lambda_{\text{max}}$ ) of **DSO**, **DCY**, **DTO** and **DPH** increase with a stronger donor ( $\lambda_{\text{max}}$  of **4** could be because the substituted amino group delocalizes the  $\pi$ -orbital more efficiently than the other groups, which results in a larger conjugated skeleton. Compared to **DSO**, **DTO** and **DPH**, **DCY** showed the smallest  $\lambda_{\text{max}}$  of 312 nm. Most importantly, unlike **DSO**, **DTO** and **DPH** with a D- $\pi$ -A architecture, **DCY** is the A- $\pi$ -A architecture.

Compared with the absorption spectra, a similar result was observed in the fluorescence spectra except that the substituent effect was larger. The emissive maximum wavelengths ( $\lambda_{\text{fl}}$ ) of four dyes increase with increasing electron-donating capacity in the

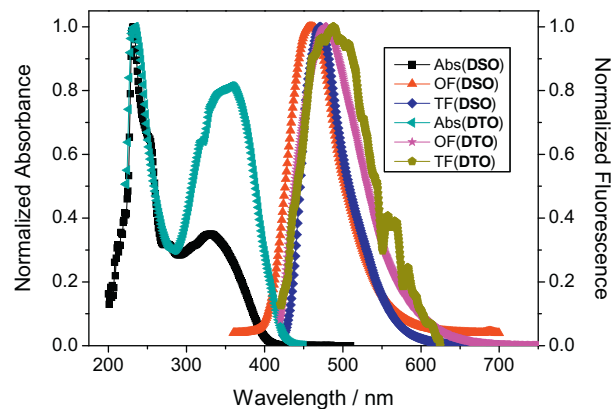


**Fig. 2.** One-photon absorption, and one- and two-photon emission spectra of **DSO** and **DTO** (1  $\mu\text{M}$ ) in CH<sub>2</sub>Cl<sub>2</sub>.

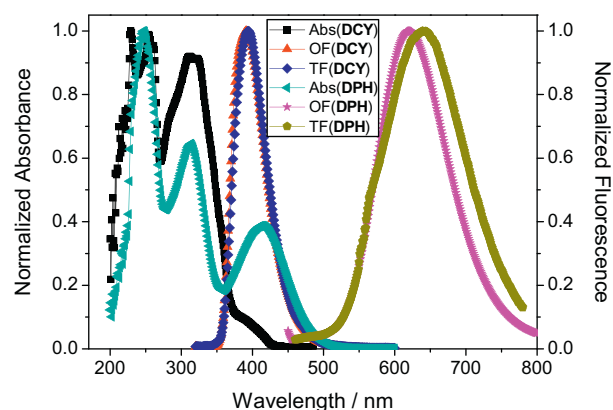


**Fig. 3.** One-photon absorption, and one- and two-photon emission spectra of **DCY** and **DPH** (1  $\mu\text{M}$ ) in CH<sub>2</sub>Cl<sub>2</sub>.

**Table 1**  
Photophysical properties of four dyes.

| Dyes | $\lambda_{\text{max}}^a$ | $\lambda_{\text{fl}}^b$ | $\Delta\nu_{\text{ST}}^c$ | $\Phi^d$ | $\lambda_{\text{max}}^{(2)e}$ | $\delta_{\text{max}}^f$ | $\tau^g$ | $\beta^h$ |
|------|--------------------------|-------------------------|---------------------------|----------|-------------------------------|-------------------------|----------|-----------|
| DSO  | 328                      | 459                     | 131                       | 0.294    | 620                           | 830                     | 0.36     | 1.2       |
| DTO  | 358                      | 479                     | 121                       | 0.320    | 700                           | 1050                    | 0.49     | 1.5       |
| DCY  | 312                      | 392                     | 80                        | 0.710    | 660                           | 1480                    | 0.68     | 2.2       |
| DPH  | 414                      | 620                     | 206                       | 0.030    | 780                           | 2800                    | 1.45     | 4.1       |

<sup>a</sup> Absorption maximum with lowest energy in nm,  $c = 10^{-5}$  M.

<sup>b</sup> Emission maximum in nm,  $c = 10^{-6}$  M.

<sup>c</sup> Stokes shift in nm.

<sup>d</sup> Relative to quinine sulfate  $10^{-6}$  M in 0.05 mol L<sup>-1</sup> H<sub>2</sub>SO<sub>4</sub>; estimated error,  $\pm 10\%$  of the given values.

<sup>e</sup> Two-photon excitation maximum in nm.

<sup>f</sup> The peak TPA cross-sections in  $10^{-50}$  cm<sup>4</sup> s/photon (GM); estimated error,  $\pm 20\%$  of the given values.

<sup>g</sup> Fluorescence lifetime in ns.

<sup>h</sup> Two-photon absorption coefficient in cm/GW.

order **DCY**, **DSO**, **DTO** and **DPH**, indicating that a stronger donor is more beneficial to intramolecular charge transfer (ICT) in the excited state, which contributes to a larger twisted angle. The larger the twisted angle, the lower the energy of the excited state, hence the emission wavelength will be larger. The Stokes shifts ( $\Delta\nu_{\text{ST}}$ ) range from 80 to 206 nm, indicating that the energy of the emitting states are significantly lower than the Franck-Condon singlet states. The  $\lambda_{\text{fl}}$  of **DPH** shows the greatest bathochromic shift and thus the largest Stokes shift in comparison to **DSO**, **DCY** and **DTO**, indicating that the donor stabilizes the lowest excited state more than the ground state (Table 1). This could be explained if the

two-photon allowed states are close to the lowest excited states. As discussed above, the donor stabilizes the latter more than the ground state to diminish the energy gap between the ground and two-photon allowed states. This would predict a higher fluorescence quantum yield, because the smaller the energy gap is, the higher the probability of the excitation will be. On the other hand, the Stokes shift decreased from **DSO** to **DTO**, probably because two methoxy groups on the side chain of **DTO** must share the cyano group acceptor to diminish the excited-state charge transfer. Most of the compounds are considerably fluorescent and the fluorescence quantum yields are close to 0.3, and even high up to 0.71 for **DCY**. The much lower quantum yield for **DPH** may be due to the sulfur atom in the phenothiazine moiety, which may facilitate the nonradiative pathways. TPF spectra are almost identical with OPF spectra.

### 3.3. Two-photon absorption cross-section and the two-photon-induced fluorescence excitation spectra

The two-photon absorption cross-section  $\delta_s$  was measured by using the two-photon-induced fluorescence measurement technique with the following equation,

$$\delta_s = \frac{S_s \eta_r \Phi_r C_r}{S_r \eta_s \Phi_s C_s} \delta_r \quad (1)$$

where the subscripts *s* and *r* stand for the sample and reference molecules, respectively [24]. The intensity of the signal collected by a PMT detector was denoted as *S*.  $\eta$  is the fluorescence quantum yield.  $\Phi$  is the overall fluorescence collection efficiency of the experimental apparatus. The number density of the molecules in solution was denoted as *C*.  $\delta_r$  is the TPA cross-section of the reference molecule.

Fig. 4 shows the two-photon-induced fluorescence excitation spectra of **DSO**, **DTO**, **DCY** and **DPH**. It can be seen that a two-photon-induced fluorescence excitation spectrum is similar to the corresponding to one-photon absorption (OPA) spectrum, and the maximum TPA wavelength ( $\lambda_{\max}^{(2)}$ ) is approximately double  $\lambda_{\max}$ . The values of the maximum  $\delta$  ( $\delta_{\max}$ ) remarkably increase in the order **DSO**, **DTO**, **DCY** and **DPH**. **DCY** with the A- $\pi$ -A architecture exhibits rather large  $\delta$  relative to **DSO** and **DTO** of D- $\pi$ -D type, which attributes to the conjugation or the orbital coupling between the terminal cyano group and the aromatic ring system. The cyano group contains the carbon-carbon triple bond (C $\equiv$ C) whose  $\pi$ -orbital can overlap with the large  $\pi$ -electron in aromatic ring, further extending  $\pi$ -conjugated system and increasing the molecular planar rigidity, which will enable a large increase in  $\delta$ .

Four dyes all exhibit rather large  $\delta$ , especially **DPH**, and even high up to 2800 GM (Table 1), which is almost larger one order of magnitude than that of the other stilbene derivatives containing no two-cyano. Therefore, the attachment of two cyano groups to the single aromatic ring of stilbene can dramatically boost the  $\delta$  value of molecules. In addition, the terminal strong electron-donating substituent such as the substitutedamino group in **DPH** is able to greatly increase  $\delta$  value. However, the alkoxy group is not satisfactory candidate. For instance, the value of even **DTO** with three methoxy groups is less than half that of **DPH**. Hence, an ideal stilbene-derived dye should be such a push-pull chromophore with the strong electron donor of the substitutedamino group at its extremity and the strong electron acceptor of two cyano groups on its single aromatic ring. The interaction between the amino group and the cyano groups can significantly improve ICT and increase the stationary dipole moment upon excitation, which drastically boosts the  $\delta$  value of the fluorophore.

Their  $\lambda_{\max}^{(2)}$  values evidently increase in the order **DSO**, **DCY**, **DTO** and **DPH**, rather than in the order **DCY**, **DSO**, **DTO** and **DPH**.

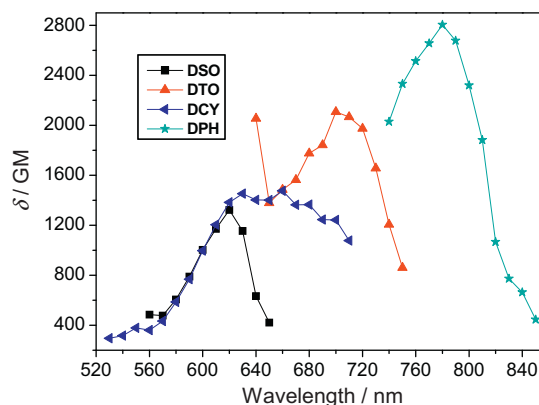


Fig. 4. Two-photon-induced fluorescence spectra for **DSO**, **DCY**, **DTO** and **DPH** (10  $\mu$ M) in  $\text{CH}_2\text{Cl}_2$  solution (with experimental error  $\sim \pm 20\%$ ).

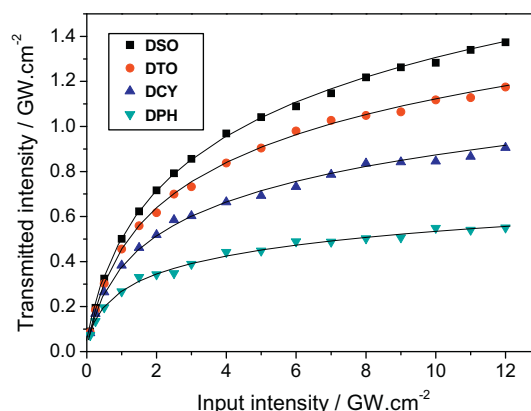


Fig. 5. Dependences of the transmitted intensities of **DSO**, **DCY**, **DTO** and **DPH** (10  $\mu$ M, in  $\text{CH}_2\text{Cl}_2$ ) on the incident intensities.

Although, among these four dyes, the  $\lambda_{\max}$ ,  $\lambda_{\text{fl}}$ , and  $\Delta\nu_{\text{ST}}$  of **DCY** are all the smallest, its  $\lambda_{\max}^{(2)}$  value exceeds that of **DSO** (Table 1), indicating the molecular planar rigidity enables  $\lambda_{\max}^{(2)}$  to bathochromically shift.

### 3.4. Optical limiting and two-photon absorption coefficient

The optical limiting experiments of **DSO**, **DTO**, **DCY** and **DPH** were performed at picosecond laser pumping. Fig. 5 shows the transmitted intensity as a function of the incident intensity for a dye ( $\text{CH}_2\text{Cl}_2$ , 10  $\mu$ M) in a 5 mm cell. Each datum was an average of 10 laser shots. We also determined the transmittance of the pure  $\text{CH}_2\text{Cl}_2$  solvent in the same 5 mm cell in order to eliminate the influences from the solvent and the cell walls. By fitting the experimental curve of transmitted intensity versus input intensity on the two-photon absorption assumption, the TPA coefficient ( $\beta$ ) of a dye can be obtained (Table 1), and the  $\beta$  value increases with increasing  $\delta$ . Similarly, their fluorescence lifetime also increases as  $\delta$  increases. The experimental data shown in Fig. 5 indicate that the optical limiting behavior of these four dyes is dominated mainly by TPA.

## 4. Conclusion

In summary, we have demonstrated the effectiveness of stilbene derivatives with two cyano groups in the single aromatic ring which can contribute to a very large  $\delta$ . The cyano group is not only

the best terminal substituent for the fluorescence quantum yield but also good for increasing  $\delta$ , while the terminal substituted amino group is the most advantageous for TPA and the bathochromic shift of the emission wavelength. The alkoxy group is the unsatisfactory candidate as the terminal group. Hence an ideal dicyanostilbene dye should contain the terminal substituted amino group. This class of dicyanostilbene dyes possess small molecule size, large  $\delta$  (830–2800 GM), long-wavelength emission (459–620 nm) and large Stokes shift (80–206 nm), and are ideal chromophores for TPF labels and probes.

### Acknowledgment

Financial supports from China Postdoctoral Science Foundation funded project (No. 20100471224) and Guangdong Natural Science Foundation (S2011040000536) is deeply acknowledged.

### Appendix A. Supplementary material

Supplementary data associated with this article can be found, in the online version, at [doi:10.1016/j.molstruc.2011.08.016](https://doi.org/10.1016/j.molstruc.2011.08.016).

### References

- [1] H.M. Kim, C. Jung, B.R. Kim, S.-Y. Jung, J.H. Hong, Y.-G. Ko, K.J. Lee, B.R. Cho, *Angew. Chem. Int. Ed.* 46 (2007) 3460.
- [2] M.K. Kim, C.S. Lim, J.T. Hong, J.H. Han, H.-Y. Jang, H.M. Kim, B.R. Cho, *Angew. Chem. Int. Ed.* 49 (2010) 364.
- [3] C.N. LaFratta, J.T. Fourkas, T. Baldacchini, R.A. Farrer, *Angew. Chem.* 119 (33) (2007) 6352.
- [4] S.-J. Jhaveri, J.-D. McMullen, R. Sijbesma, L.-S. Tan, W. Zipfel, C.-K. Ober, *Chem. Mater.* 21 (10) (2009) 2003.
- [5] S.-H. Park, D.-Y. Yang, K.-S. Lee, *Laser Photon. Rev.* 3 (1–2) (2009) 1.
- [6] K.D. Belfield, K.J. Schafer, *Chem. Mater.* 14 (9) (2002) 3656.
- [7] C.O. Yanez, C.D. Andrade, S. Yao, G. Luchita, M.V. Bondar, K.D. Belfield, *ACS Appl. Mater. Interfaces* 1 (2009).
- [8] S.L. Oliveira, D.S. Correa, L. Misoguti, C.J.L. Constantino, R.F. Aroca, S.C. Zilio, C.R. Mendonca, *Adv. Mater.* 17 (15) (2005) 1890.
- [9] T.-C. Lin, S.-J. Chung, K.S. Kim, X. Wang, G.S. He, J. Swiatkiewicz, H.E. Pudavar, P.N. Prasad, *Adv. Polym. Sci.* 161 (2003) 157.
- [10] M. Velusamy, J.-Y. Shen, J.-T. Lin, Y.-C. Lin, C.-C. Hsieh, C.-H. Lai, C.-W. Lai, M.-L. Ho, Y.-H. Chen, P.-T. Chou, J.-K. Hsiao, *Adv. Funct. Mater.* 19 (15) (2009) 2388.
- [11] C.-F. Peter, *Acc. Chem. Res.* 41 (2) (2008) 190.
- [12] G.C.R. Ellis-Davies, *Nat. Methods* 4 (2007) 619.
- [13] J.E. Ehrlich, X.L. Wu, I.-Y.S. Lee, Z.-Y. Hu, H. Röckel, S.R. Marder, J.W. Perry, *Opt. Lett.* 22 (24) (1997) 1843.
- [14] Z. Liu, Q. Fang, D. Wang, D. Cao, G. Xue, W. Yu, H. Lei, *Chem. Eur. J.* 9 (2003) 5074.
- [15] W.J. Yang, D.Y. Kim, C.H. Kim, M.Y. Jeong, S.K. Lee, S.J. Jeon, B.R. Cho, *Org. Lett.* 6 (9) (2004) 1389.
- [16] S.J.K. Pond, M. Rumi, M.D. Levin, T.C. Parker, D. Beljonne, M.W. Day, J.-L. Brédas, S.R. Marder, J.W. Perry, *J. Phys. Chem. A* 106 (2002) 11470.
- [17] C. Huang, A. Ren, C. Feng, N. Yang, *Sens. Actuators B: Chem.* 151 (1) (2010) 236.
- [18] C. Huang, J. Fan, X. Peng, Z. Lin, B. Guo, A. Ren, J. Cui, S. Sun, *J. Photochem. Photobiol. A* 199 (2008) 144.
- [19] D.F. Eaton, *J. Photochem. Photobiol. B* 2 (1988) 523.
- [20] C. Xu, W.W. Webb, *J. Opt. Soc. Am. B* 13 (1996) 481.
- [21] S.C. Burdette, G.K. Walkup, B. Spingler, R.Y. Tsien, S.J. Lippard, *J. Am. Chem. Soc.* 123 (2001) 7831.
- [22] H. Huang, Q. He, H. Lin, F. Bai, Z. Sun, Q. Li, *Polym. Adv. Technol.* 15 (2004) 84.
- [23] Y. Zou, W. Wu, G. Sang, Y. Yang, Y. Liu, Y. Li, *Macromolecules* 40 (2007) 7231.
- [24] S.J.K. Pond, O. Tsutsumi, M. Rumi, O. Kwon, E. Zojer, J.L. Brédas, S.R. Marder, J.W. Perry, *J. Am. Chem. Soc.* 126 (30) (2004) 9291.